

Supporting Information

J. Chem. Metrol. X:X (2021) XX-XX

Isolation of amygdalin epimer at high diastereomeric purity and its structural characterization by spectroscopic and Q-TOF LC-MS methods

Pshtiwan Raheem Sabır ¹, İrfan Çapan ^{2,3*}, Ayhan İbrahim Aysal ³ and Süleyman Servi ⁴

¹ Garmian University, College of Education, Chemistry Department, Kalar, Sulaymanyah-Iraq

^{2*} Gazi University, Technical Sciences Vocational College, Department of Polymer Technology, 06560 Ankara-Türkiye

³ Gazi University, Faculty of Pharmacy, Department of Pharmaceutical Chemistry, Ankara- Türkiye

⁴ Fırat University, Faculty of Science, Department of Chemistry, 23169 Elazığ- Türkiye

Table of Contents	Page
Figure S1: Liquid-Liquid Extractions (LLE); A = n-hexane, B = petroleum ether, C = chloroform	3
Figure S2: D = n-hexane, E = petroleum ether, F = chloroform	3
Figure S3: ATR-IR spectrum of the amygdalin-free component of the extract	3
Figure S4: ¹ H-NMR (400 MHz, CDCl ₃) spectrum of the amygdalin-free component of the extract	3
Figure S5: ¹³ C-NMR (400 MHz, CDCl ₃) spectrum of the amygdalin-free component of the extract	4
Figure S6: (A) ATR-FTIR spectrum of the extract obtained without any purification operations; (B) ATR-FTIR spectrum of the isolated amygdalin at high diastereomeric purity	5
Figure S7: O-H bonds region of amygdalin	5
Figure S8: Nitrile region of amygdalin	5
Figure S9: C-O-H and C-O-C bond region of amygdalin	6
Figure S10: Numbering system used to evaluate NMR spectra of amygdalin. It is not related to the IUPAC numbering system	6

Figure S11: 1 H-NMR (400 MHz, DMSO-d ₆) spectrum of the extract obtained after LLE	7
Figure S12: 13 C-NMR (100 MHz, DMSO-d ₆) spectrum of the extract obtained after LLE	7
Figure S13: 1H-NMR (400 MHz, DMSO-d ₆) spectrum of the amygdalin isolated at high purity after column chromatography	8
Figure S14: The 1H-NMR (400 MHz, D ₂ O) spectrum of the amygdalin after column chromatography	9
Figure S15: 13C-NMR (100 MHz, D ₂ O) spectrum of the amygdalin isolated after column chromatography	10
Figure S16: 13C-NMR (100 MHz, DMSO-d ₆) spectrum of the amygdalin isolated at high purity column chromatography	11
Figure S17: The UV-VIS spectrum of the isolated pure amygdalin.	11
Figure S18: TIC of the sample in MS-MS mode	11
Figure S19: MS spectrum of peak at RT 1.41	11
Figure S20: Isotopic distribution of 456 ion at RT 1.42 showing experimental and calculated values	12
Figure S21: MS spectrum of peak at RT 4.17	12
Figure S22: Isotopic distribution of 456 ion at RT 4.17	12



Figure S1: Liquid-Liquid Extractions (LLE); A = n-hexane, B = petroleum ether, C = chloroform

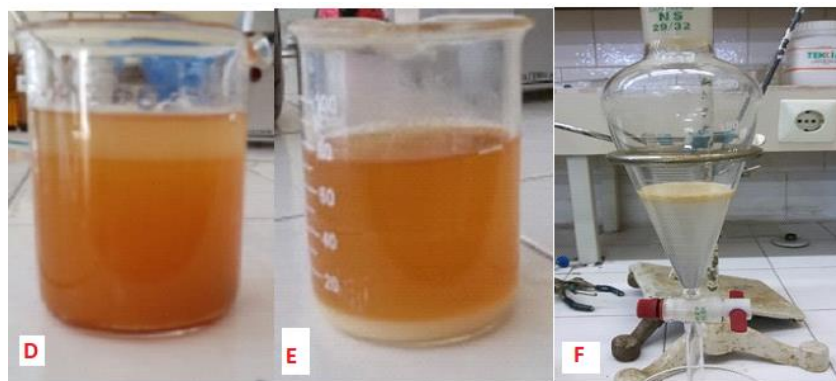


Figure S2: Decantation Methods; D = n-hexane, E = petroleum ether, F = chloroform

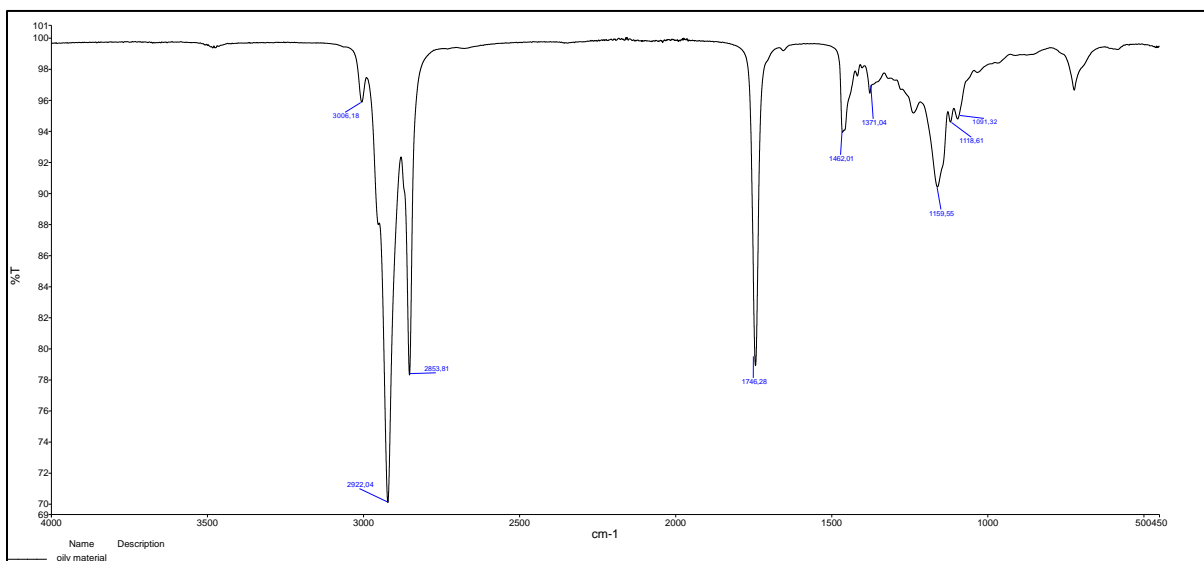


Figure S3: ATR-IR spectrum of the amygdalin-free component of the extract

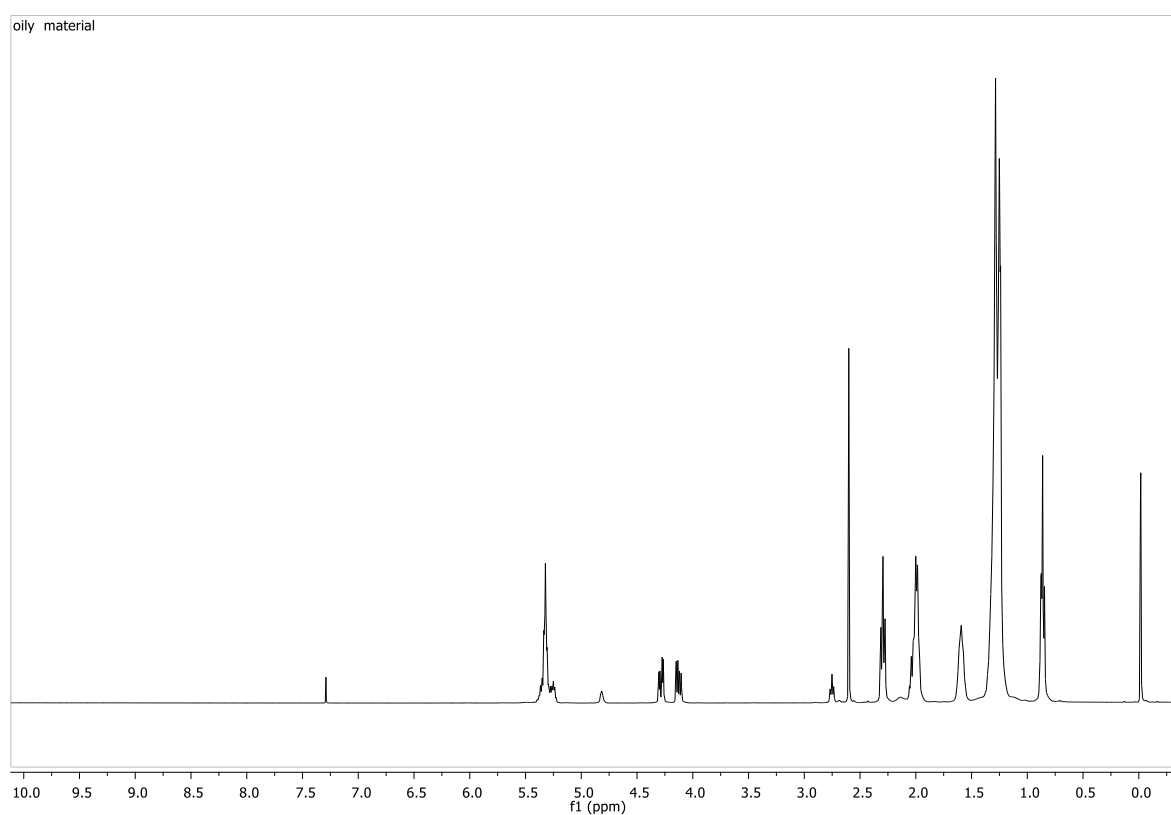


Figure S4: $^1\text{H-NMR}$ (400 MHz, CDCl_3) spectrum of the amygdalin-free component of the extract

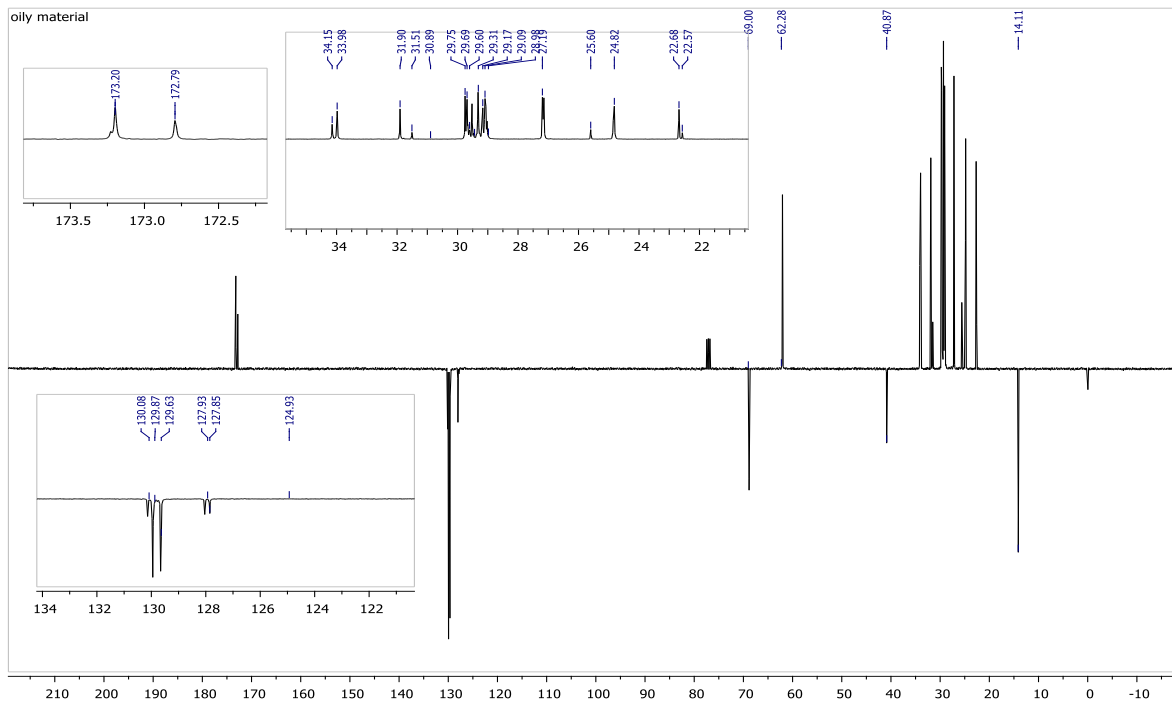


Figure S5: ^{13}C -NMR (400 MHz, CDCl_3) spectrum of the amygdalin-free component of the extract

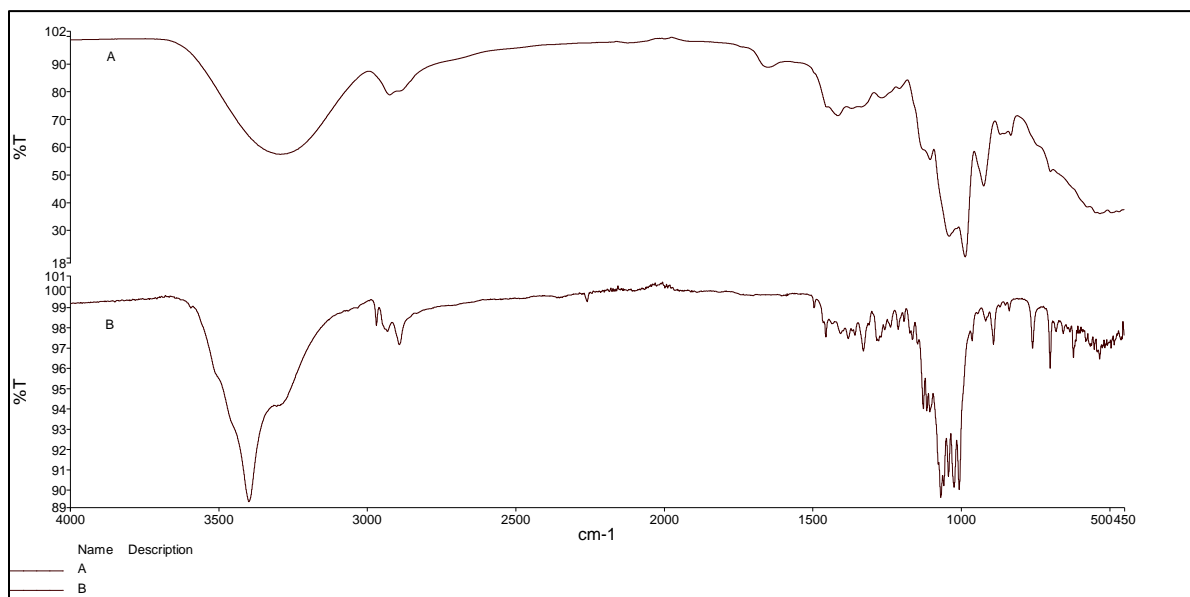


Figure S6 :(A) ATR-FTIR spectrum of the extract obtained without any purification operations; (B) ATR-FTIR spectrum of the isolated amygdalin at high diastereomeric purity

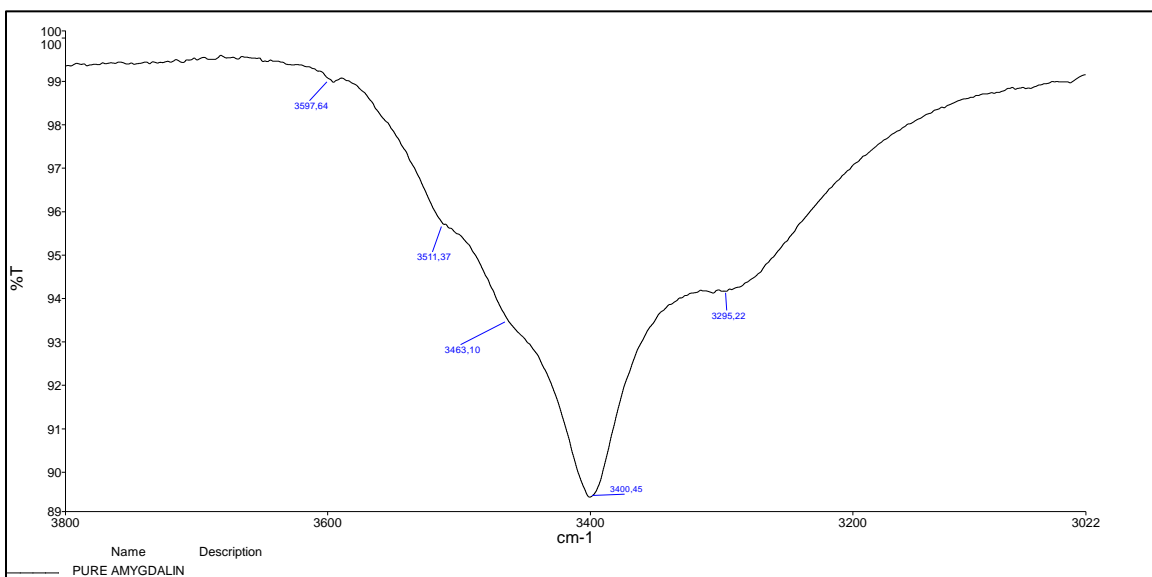


Figure S7: O-H bonds region of amygdalin

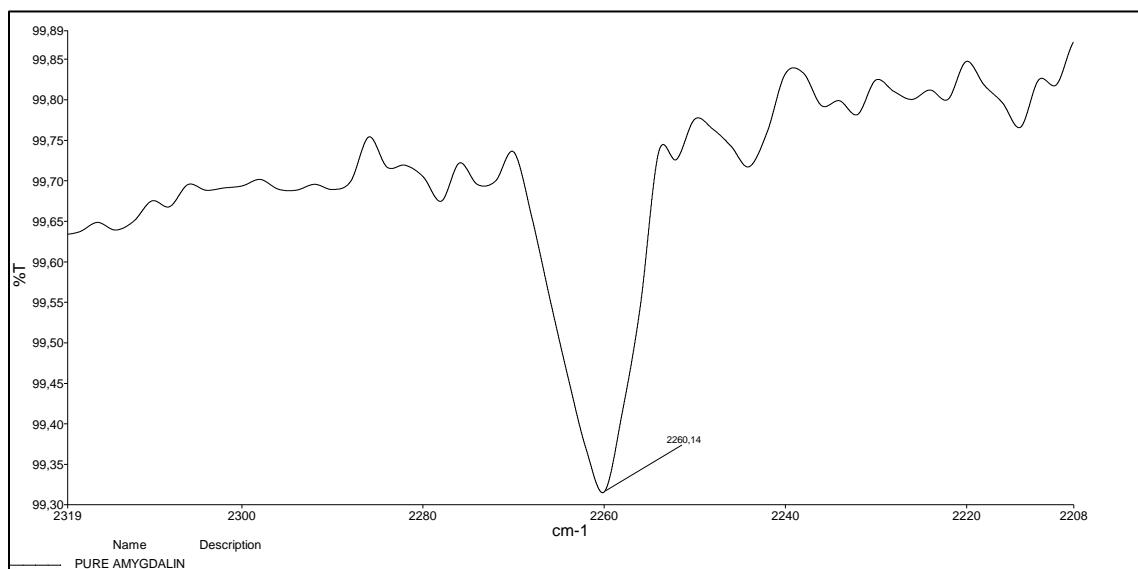


Figure S8: Nitrile region of amygdalin

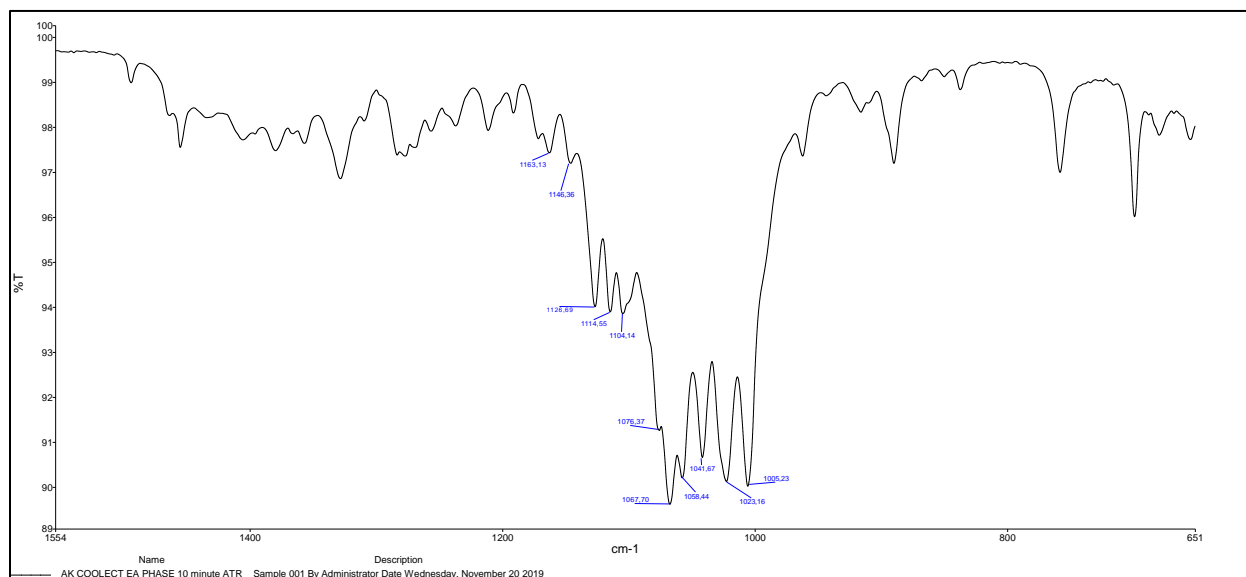


Figure S9: C-O-H and C-O-C bond region of amygdalin

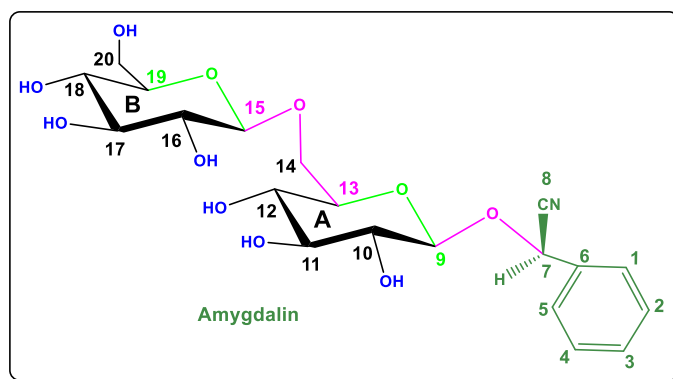


Figure S10: Numbering system used to evaluate NMR spectra of amygdalin. It is not related to the IUPAC numbering system

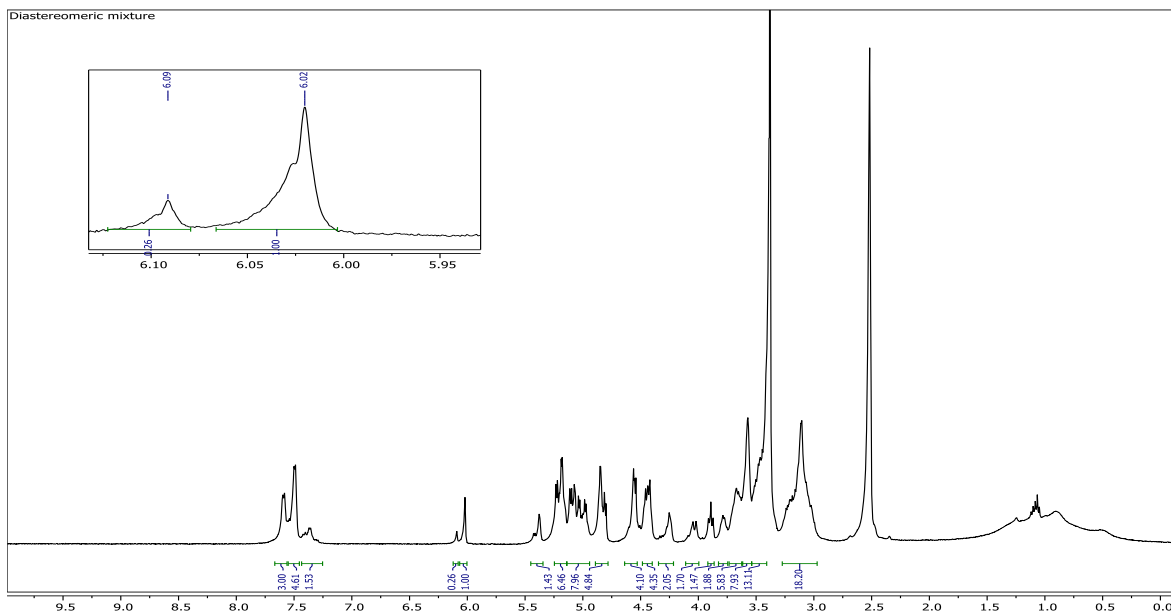


Figure S11: $^1\text{H-NMR}$ (400 MHz, DMSO-d_6) spectrum of the extract obtained after LLE

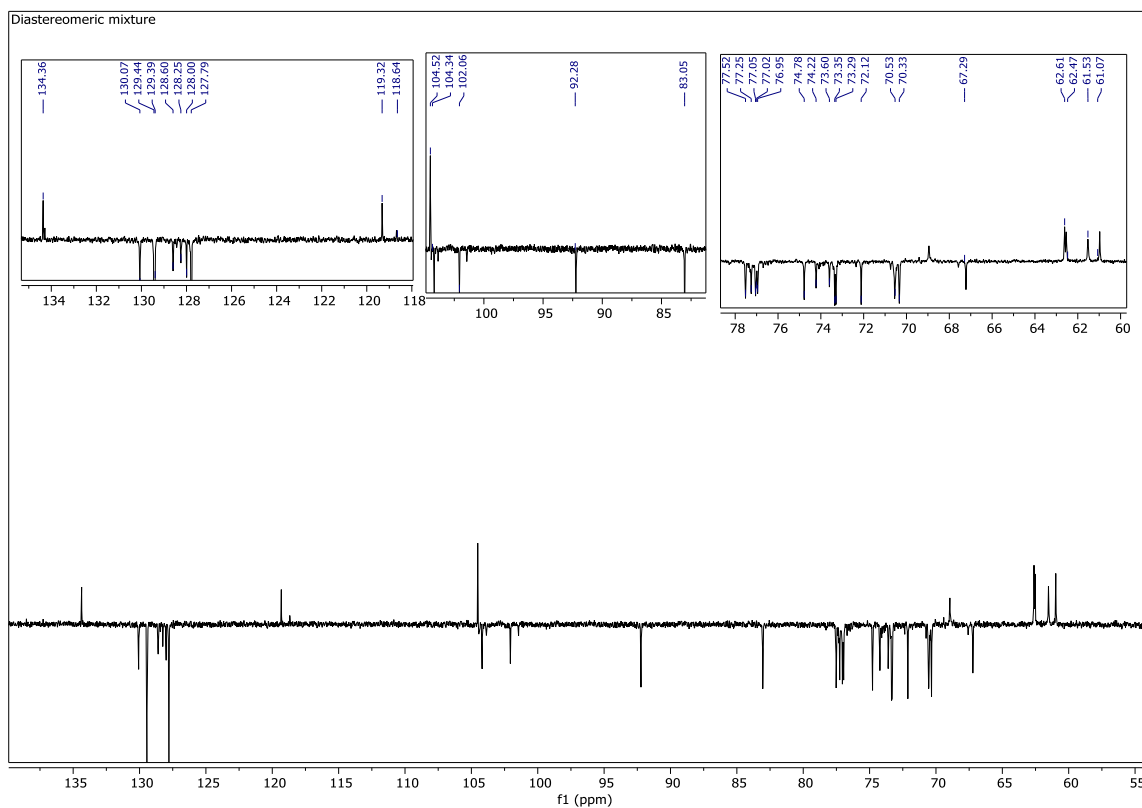


Figure S12: $^{13}\text{C-NMR}$ (100 MHz, DMSO-d_6) spectrum of the extract obtained after LLE

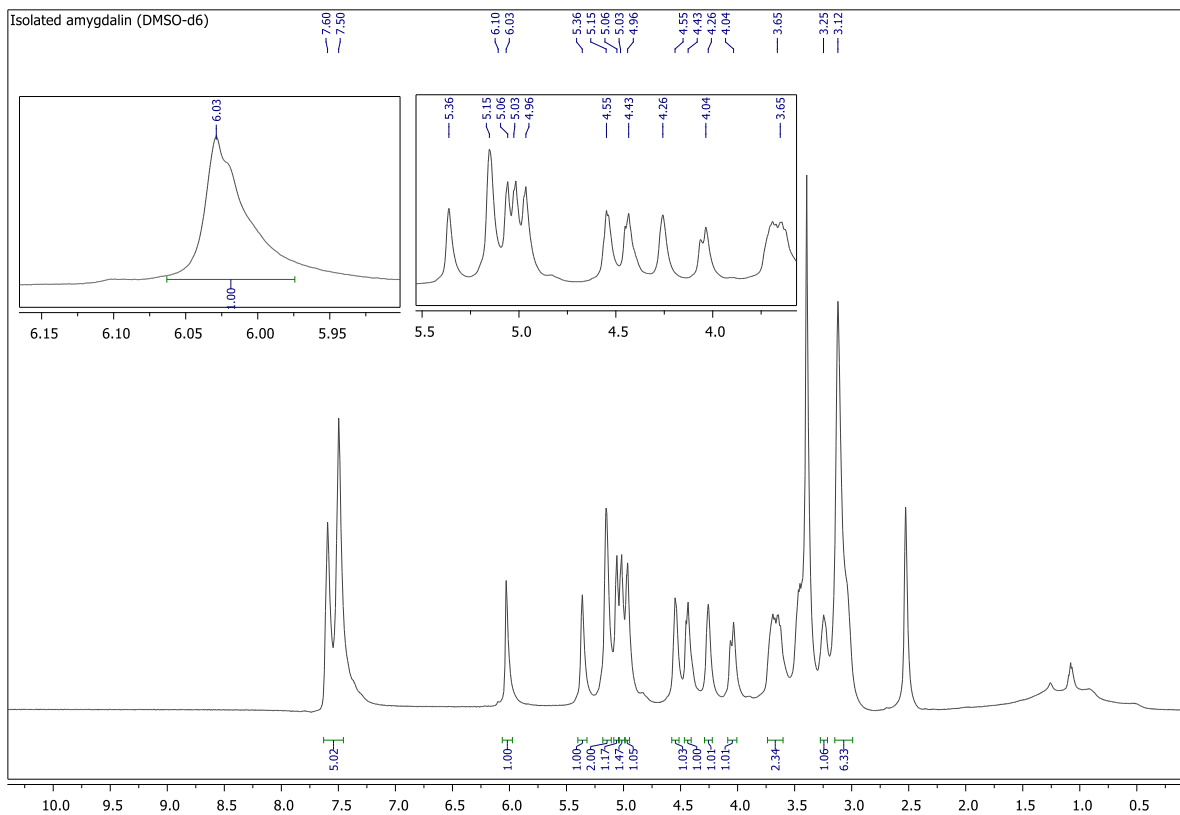


Figure S13: ^1H -NMR (400 MHz, DMSO-d₆) spectrum of the amygdalin isolated at high purity after column chromatography

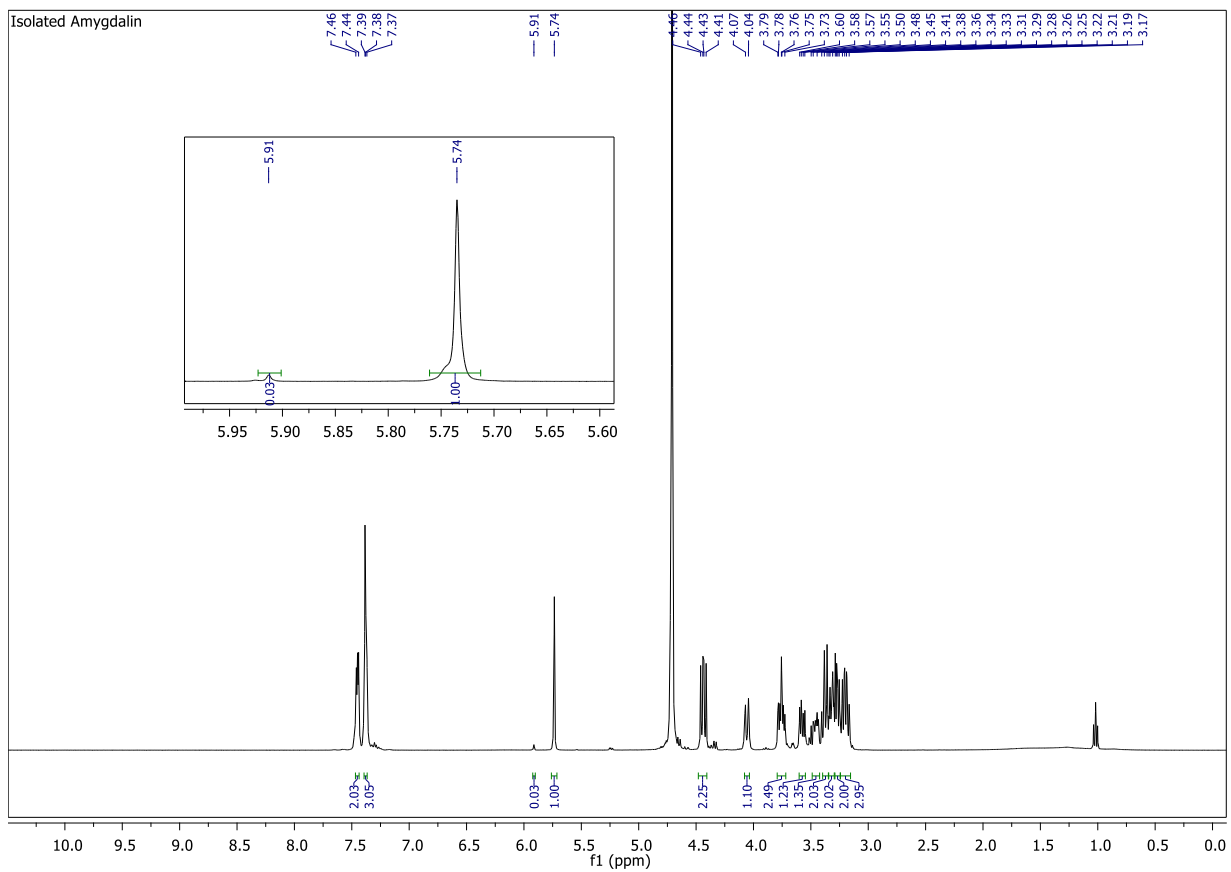


Figure S14: The $^1\text{H-NMR}$ (400 MHz, D_2O) spectrum of the amygdalin after column chromatography

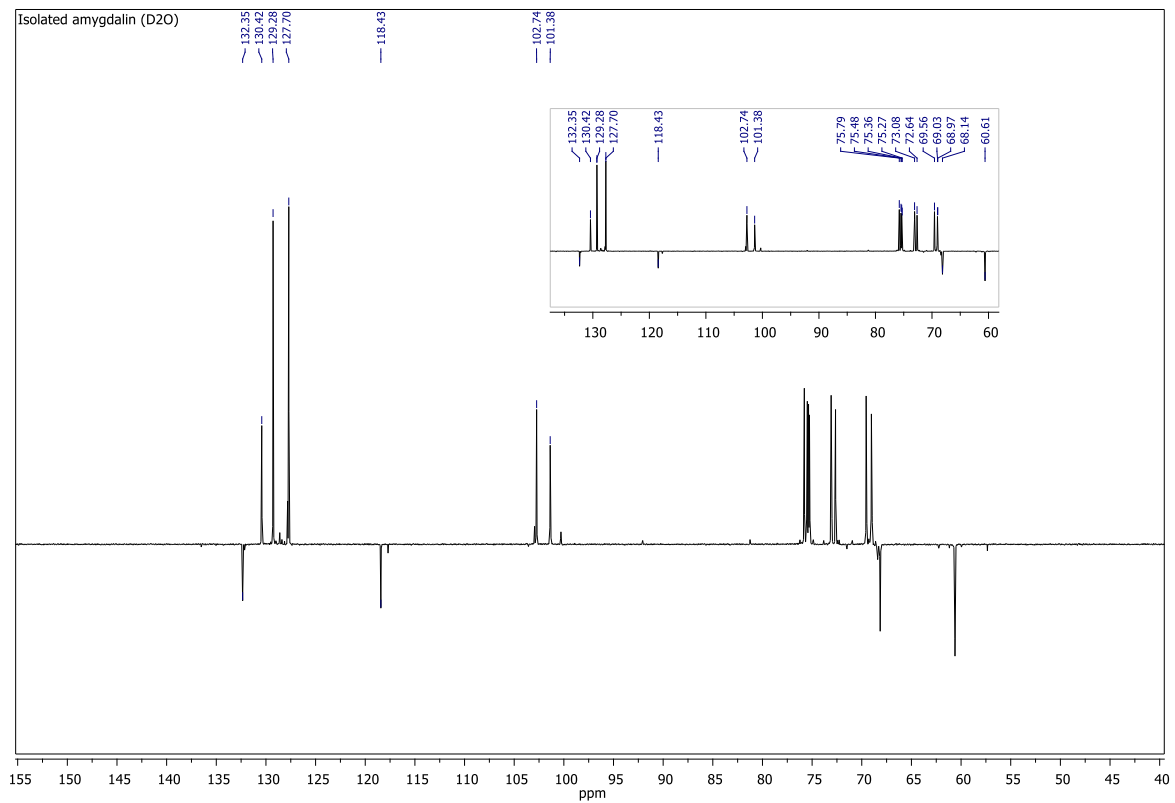
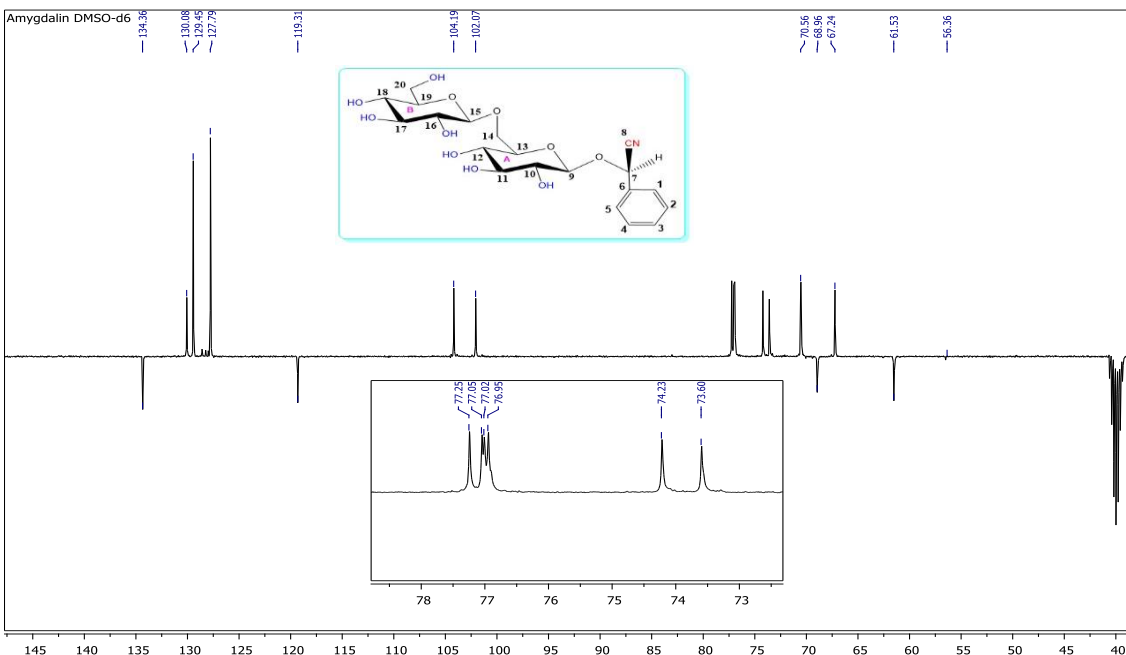


Figure S15: ¹³C-NMR (100 MHz, D₂O) spectrum of the amygdalin isolated after column chromatography



Figure

S16: ¹³C-NMR (100 MHz, DMSO-d₆) spectrum of the amygdalin isolated at high purity column chromatography

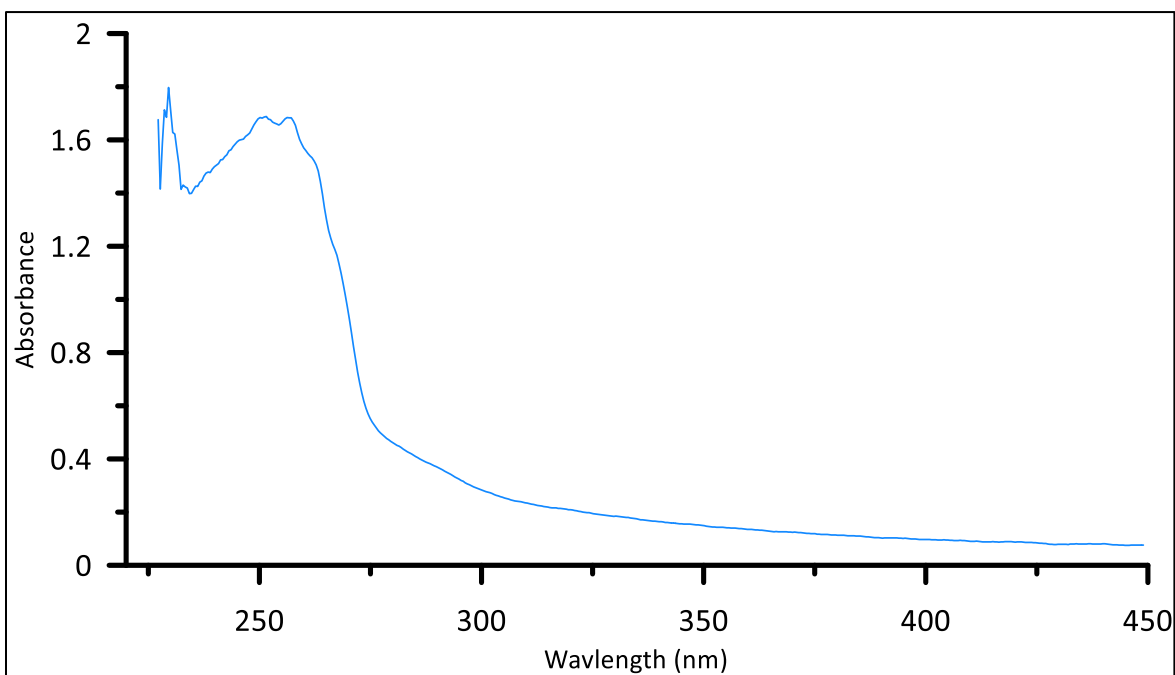


Figure S17: The UV-VIS spectrum of the isolated pure amygdalin.

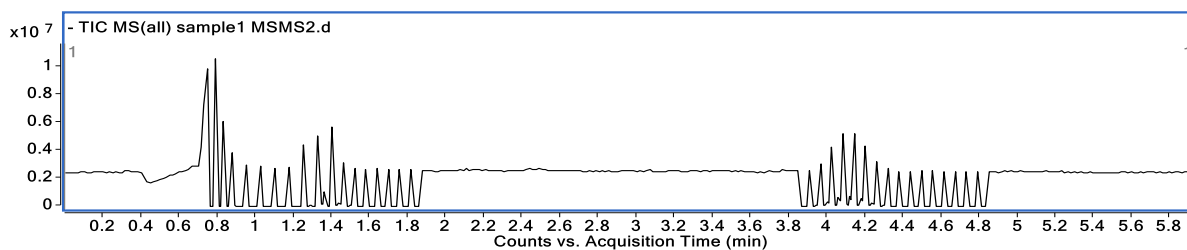


Figure S18: TIC of the sample in MS-MS mode

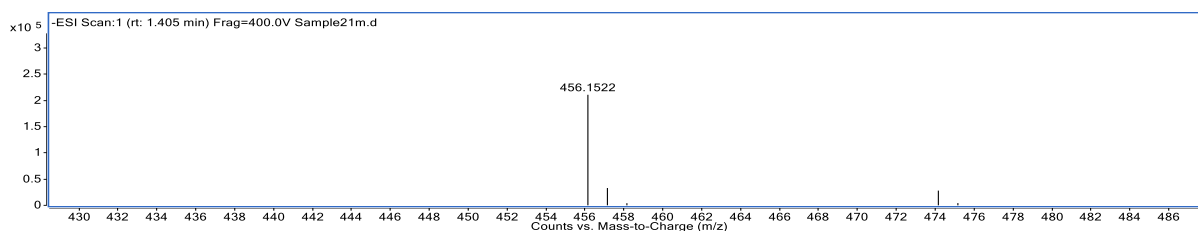


Figure S19: MS spectrum of peak at RT 1.41

Spectrum Identification Results - Scan:1 (rt: 1.405 min)

Best	ID Source	Name	Formula	Species	m/z	Score	Diff (ppm)	Score (MFG)	Mass
			C ₂₀ H ₂₇ N O ₁₁	(M-H) ⁻	456.1522	87.71	-2.09	87.71	457.1594
Score (iso. abund)	Score (mass)	Score (MFG, MS/MS)	Score (MS)	Score (MFG)	Score (iso. spacing)	Height	Ion Formula	Species	m/z
65.46	95.68	87.71	87.71	98.47	210776.2	C ₂₀ H ₂₆ N O ₁₁	(M-H) ⁻	456.1522	
Height (Calc)	Height Sum% (Calc)	Height % (Calc)	m/z (Calc)	Diff (mDa)	Height	Height %	Height Sum %	m/z	Diff (ppm)
194524.4	78.5	100	456.1511	-1.1	210776.2	100	85	456.1522	-2.31
44185.9	17.8	22.7	457.1544	-0.4	33032.2	15.7	13.3	457.1549	-0.96
9186.5	3.7	4.7	458.1566	-0.1	4088.5	1.9	1.6	458.1567	-0.23

Figure S20. Isotopic distribution of 456 ion at RT 1.42 showing experimental and calculated values

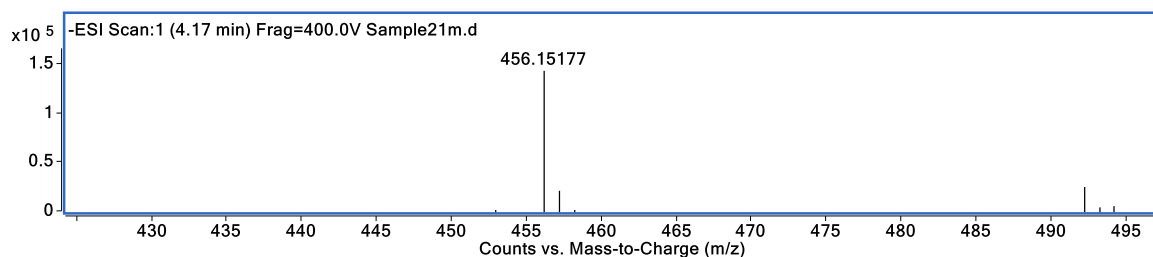


Figure S21: MS spectrum of peak at RT 4.17

Spectrum Identification Results - Scan:1 (4.17 min)												
Automatically Show Columns												
Best	ID Source	Name	Formula	Species	m/z	Score	Score (RT)	RT Diff	Diff (ppm)	Score (Lib)	Score (DB)	Score (MFG)
	MFG		C20 H27 N O11	(M-H)-	456.15177	88.09			-1.16			88.09
Species	m/z	Score (iso. abund)	Score (mass)	Score (MFG, MS/MS)	Score (MS)	Score (MFG)	Score (iso. spacing)	Height	Ion Formula			
(M-H)-	456.15177	61.88	98.65		88.09	88.09	98.43	143313.3	C20 H26 N O11			
Height (Calc)	Height Sum% (Calc)	Height % (Calc)	m/z (Calc)	Diff (mDa)	Height	Height %	Height Sum %	m/z	Diff (ppm)			
131868.8	78.5	100	456.15113	-0.6	143313.3	100	85.3	456.15177	-1.4			
29953.8	17.8	22.7	457.15444	0	21704	15.1	12.9	457.15448	-0.08			
6227.6	3.7	4.7	458.15661	0.9	3032.9	2.1	1.8	458.15672	1.94			

Figure S22: Isotopic distribution of 456 ion at RT 4.17